EUROPEAN ORGANISATION FOR NUCLEAR RESEARCH

CERN-PPE/90-116
14 August 1990

Limits on a Light Higgs Boson in e^+e^- Collisions at LEP

The OPAL Collaboration

Abstract

Data from e^+e^- collisions collected with the OPAL detector at LEP have been used to exclude a Standard Model Higgs boson (H^0) with mass below $2m_\mu$. The analysis used 1.2 pb^{-1} of data taken at centre-of-mass energies between 88.3 and 95.0 GeV to search for the reactions $e^+e^- \to Z^0H^0, (Z^0 \to e^+e^-$ or $\mu^+\mu^-, H^0 \to$ *undetected*), $e^+e^- \to Z^0H^0, (Z^0 \to \nu\bar{\nu}, H^0 \to e^+e^-$ or $\gamma\gamma)$. The existence of a minimal Standard Model H^0 with mass in the range $0 \leq m_H \leq 2m_\mu$ is excluded at the 95% confidence level. The limit is also valid for Standard Model extensions with a large branching ratio for the decay of H^0 to $\gamma\gamma$.

(Submitted to Physics Letters B)

The OPAL Collaboration

M.Z. Akrawy[11], G. Alexander[21], J. Allison[14], P.P. Allport[5], K.J. Anderson[8], J.C. Armitage[6], G.T.J. Arnison[18], P. Ashton[14], G. Azuelos[16,f], J.T.M. Baines[14], A.H. Ball[15], J. Banks[14], G.J. Barker[11], R.J. Barlow[14], J.R. Batley[5], A. Beck[21], J. Becker[9], T. Behnke[7], K.W. Bell[18], G. Bella[21], S. Bethke[10], O. Biebel[3], U. Binder[9], I.J. Bloodworth[1], P. Bock[10], H. Breuker[7], R.M. Brown[18], R. Brun[7], A. Buijs[7], H.J. Burckhart[7], P. Capiluppi[2], R.K. Carnegie[6], A.A. Carter[11], J.R. Carter[8], C.Y. Chang[15], D.G. Charlton[7], J.T.M. Chrin[14], P.E.L. Clarke[23], I. Cohen[21], W.J. Collins[5], J.E. Conboy[13], M. Couch[1], M. Coupland[12], M. Cuffiani[2], S. Dado[20], G.M. Dallavalle[2], P. Debu[19], M.M. Deninno[2], A. Dieckmann[10], M. Dittmar[4], M.S. Dixit[17], E. Duchovni[24], I.P. Duerdoth[7,d], D.J.P. Dumas[6], H. El Mamouni[16], P.A. Elcombe[5], P.G. Estabrooks[6], E. Etzion[21], F. Fabbri[2], P. Farthouat[19], H.M. Fischer[3], D.G. Fong[15], M.T. French[18], C. Fukunaga[22], A. Gaidot[19], O. Ganel[24], J.W. Gary[10], J. Gascon[16], N.I. Geddes[18], C.N.P. Gee[18], C. Geich-Gimbel[3], S.W. Gensler[8], F.X. Gentit[19], G. Giacomelli[2], V. Gibson[5], W.R. Gibson[11], J.D. Gillies[18], J. Goldberg[20], M.J. Goodrick[5], W. Gorn[4], D. Granite[20], E. Gross[24], J. Grunhaus[21], H. Hagedorn[9], J. Hagemann[7], M. Hansroul[7], C.K. Hargrove[17], I. Harrus[20], J. Hart[5], P.M. Hattersley[1], M. Hauschild[7], C.M. Hawkes[7], E. Heflin[4], R.J. Hemingway[6], R.D. Heuer[7], J.C. Hill[5], S.J. Hillier[1], C. Ho[4], J.D. Hobbs[8], P.R. Hobson[23], D. Hochman[24], B. Holl[7], R.J. Homer[1], S.R. Hou[15], C.P. Howarth[13], R.E. Hughes-Jones[14], R. Humbert[9], P. Igo-Kemenes[10], H. Ihssen[10], D.C. Imrie[23], L. Janissen[6], A. Jawahery[15], P.W. Jeffreys[18], H. Jeremie[16], M. Jimack[7], M. Jobes[1], R.W.L. Jones[11], P. Jovanovic[1], D. Karlen[6], K. Kawagoe[22], T. Kawamoto[22], R.G. Kellogg[15], B.W. Kennedy[13], C. Kleinwort[7], D.E. Klem[17], G. Knop[3], T. Kobayashi[22], T.P. Kokott[3], L. Köpke[7], R. Kowalewski[6], H. Kreutzmann[3], J. Kroll[8], M. Kuwano[22], P. Kyberd[11], G.D. Lafferty[14], F. Lamarche[16], W.J. Larson[4], J.G. Layter[4], P. Le Du[19], P. Leblanc[16], A.M. Lee[15], M.H. Lehto[13], D. Lellouch[7], P. Lennert[10], L. Lessard[16], L. Levinson[24], S.L. Lloyd[11], F.K. Loebinger[14], J.M. Lorah[15], B. Lorazo[16], M.J. Losty[17], J. Ludwig[9], J. Ma[4,b], A.A. Macbeth[14], M. Mannelli[7], S. Marcellini[2], G. Maringer[3], A.J. Martin[11], J.P. Martin[16], T. Mashimo[22], P. Mättig[7], U. Maur[3], T.J. McMahon[1], J.R. McNutt[23], F. Meijers[7], D. Menszner[10], F.S. Merritt[8], H. Mes[17], A. Michelini[7], R.P. Middleton[18], G. Mikenberg[24], J. Mildenberger[6], D.J. Miller[13], C. Milstene[21], M. Minowa[22], W. Mohr[9], A. Montanari[2], T. Mori[22], M.W. Moss[14], P.G. Murphy[14], W.J. Murray[5], B. Nellen[3], H.H. Nguyen[8], M. Nozaki[22], A.J.P. O'Dowd[14], S.W. O'Neale[7,e], B.P. O'Neill[4], F.G. Oakham[17], F. Odorici[2], M. Ogg[6], H. Oh[4], M.J. Oreglia[8], S. Orito[22], J.P. Pansart[19], G.N. Patrick[18], S.J. Pawley[14], P. Pfister[9], J.E. Pilcher[8], J.L. Pinfold[24], D.E. Plane[7], B. Poli[2], A. Pouladdej[6], E. Prebys7, T.W. Pritchard[11], G. Quast[7], J. Raab[7], M.W. Redmond[8], D.L. Rees[1], M. Regimbald[16], K. Riles[4], C.M. Roach[5], S.A. Robins[11], A. Rollnik[3], J.M. Roney[8], S. Rossberg[9], A.M. Rossi[2,a], P. Routenburg[6], K. Runge[9], O. Runolfsson[7], S. Sanghera[6], R.A. Sansum[18], M. Sasaki[22], B.J. Saunders[18], A.D. Schaile[9], O. Schaile[9], W. Schappert[6], P. Scharff-Hansen[7], S. Schreiber[3], J. Schwarz[9], A. Shapira[24], B.C. Shen[4], P. Sherwood[13], A. Simon[3], P. Singh[11], G.P. Siroli[2], A. Skuja[15], A.M. Smith[7], T.J. Smith[1], G.A. Snow[15], R.W. Springer[15], M. Sproston[18], K. Stephens[14], H.E. Stier[9], R. Stroehmer[10], D. Strom[8], H. Takeda[22], T. Takeshita[22], N.J. Thackray[1], T. Tsukamoto[22], M.F. Turner[5], G. Tysarczyk-Niemeyer[10], D. Van den plas[16], G.J. VanDalen[4], G. Vasseur[19], C.J. Virtue[17], H. von der Schmitt[10], J. von Krogh[10], A. Wagner[10], C. Wahl[9], J.P. Walker[1], C.P. Ward[5], D.R. Ward[5], P.M. Watkins[1], A.T. Watson[1], N.K. Watson[1], M. Weber[10], S. Weisz[7], P.S. Wells[7], N. Wermes[10], M. Weymann[7], G.W. Wilson[19], J.A. Wilson[1], I. Wingerter[7], V-H. Winterer[9], N.C. Wood[13], S. Wotton[7], B. Wuensch[3], T.R. Wyatt[14], R. Yaari[24], Y. Yang[4,b], G. Yekutieli[24], T. Yoshida[22], W. Zeuner[7], G.T. Zorn[15].

[1]School of Physics and Space Research, University of Birmingham, Birmingham, B15 2TT, UK
[2]Dipartimento di Fisica dell' Università di Bologna and INFN, Bologna, 40126, Italy
[3]Physikalisches Institut, Universität Bonn, D-5300 Bonn 1, FRG
[4]Department of Physics, University of California, Riverside, CA 92521 USA
[5]Cavendish Laboratory, Cambridge, CB3 0HE, UK
[6]Carleton University, Dept of Physics, Colonel By Drive, Ottawa, Ontario K1S 5B6, Canada
[7]CERN, European Organisation for Particle Physics, 1211 Geneva 23, Switzerland
[8]Enrico Fermi Institute and Department of Physics, University of Chicago, Chicago Illinois 60637, USA
[9]Fakultät für Physik, Albert Ludwigs Universität, D-7800 Freiburg, FRG
[10]Physikalisches Institut, Universität Heidelberg, Heidelberg, FRG
[11]Queen Mary and Westfield College, University of London, London, E1 4NS, UK
[12]Birkbeck College, London, WC1E 7HV, UK
[13]University College London, London, WC1E 6BT, UK
[14]Department of Physics, Schuster Laboratory, The University, Manchester, M13 9PL, UK
[15]Department of Physics and Astronomy, University of Maryland, College Park, Maryland 20742, USA
[16]Laboratoire de Physique Nucléaire, Université de Montréal, Montréal, Quebec, H3C 3J7, Canada
[17]National Research Council of Canada, Herzberg Institute of Astrophysics, Ottawa, Ontario K1A 0R6, Canada
[18]Rutherford Appleton Laboratory, Chilton, Didcot, Oxfordshire, OX11 0QX, UK
[19]DPhPE, CEN Saclay, F-91191 Gif-sur-Yvette, France
[20]Department of Physics, Technion-Israel Institute of Technology, Haifa 32000, Israel
[21]Department of Physics and Astronomy, Tel Aviv University, Tel Aviv 69978, Israel
[22]International Centre for Elementary Particle Physics and Dept of Physics, University of Tokyo, Tokyo 113, and Kobe University, Kobe 657, Japan
[23]Brunel University, Uxbridge, Middlesex, UB8 3PH UK
[24]Nuclear Physics Department, Weizmann Institute of Science, Rehovot, 76100, Israel

[a]Present address: Dipartimento di Fisica, Università della Calabria, 87036 Rende, Italy
[b]On leave from Harbin Institute of Technology, Harbin, China
[c]Now at Applied Silicon Inc
[d]On leave from Manchester University
[e]On leave from Birmingham University
[f]and TRIUMF, Vancouver, Canada

1 Introduction

An essential aspect of the Standard Model of electroweak interactions [1] is the mechanism of spontaneous symmetry breaking which gives masses to the $W^{\pm}$ and Z^0 bosons and fundamental fermions. The existence of a single physical neutral scalar boson, the Higgs boson [2], and its couplings to the intermediate vector bosons, quarks and leptons are intrinsic predictions of the symmetry breaking part of the minimal model. Its mass, however, is not predicted, and to date the Higgs boson has eluded experimental observation.

An indirect limit on the Higgs mass based on vacuum stability arguments [3,4] has been derived from the limits on the top quark mass and searches for a Higgs boson with mass less than twice the muon mass (m_μ) have been performed in a number of experiments prior to the commissioning of the LEP accelerator. These include studies of transitions in muonic atoms [5], nuclear transition rates [6,7], neutron-nucleon scattering[8], rare kaon decays [9,10,11], and the decay $\pi^+ \rightarrow e^+\nu_e e^+e^-$ [12]. These analyses depend on theoretical assumptions related to the Higgs-nucleon coupling, hadronic contributions to kaon decays, or the gluonic content of the pion [9,13,14]. Free of theoretical uncertainties is a search for electron bremsstrahlung of Higgs bosons in an electron beam-dump experiment [15] which excludes a Higgs boson decaying to e^+e^- in the range $1.2 \leq m_H \leq 52$ MeV/c^2 at the 90% confidence level.

The results of a search for the Higgs boson in the mass range $0 \leq m_H \leq 2\ m_\mu$ presented here rely only on the fundamental couplings of the Standard Model. If such a light Higgs boson exists it would be produced at LEP energies through the reaction $e^+e^- \rightarrow Z^0 \rightarrow H^0Z^0$. This process involves the coupling of three point-like particles (ZHZ) which can be calculated exactly within the framework of the Standard Model. $\Gamma(Z^0 \rightarrow Z^0H^0)/\Gamma(Z^0 \rightarrow \mathit{anything})$ is predicted to be of the order of 10^{-2} [16] for $0 \leq m_H \leq 2\ m_\mu$. The only visible decay modes in this mass range are $H^0 \rightarrow e^+e^-$ and $H^0 \rightarrow \gamma\gamma$. The former is strongly favoured for $2m_e < m_H < 2m_\mu$ in the Standard Model assuming three generations but the latter can become significant in this mass range in some extensions of the model. In particular, very large enhancements occur in models containing more than three generations [16]. Long-lived Higgs bosons, or Higgs bosons that decay to light neutrinos or light supersymmetric particles, may not be visible inside the detector and would only be detectable via the decay products of the associated Z^0.

In order to include all decay modes of the Higgs with mass less than $2m_\mu$, a search for the following processes has been performed:

$$e^+e^- \rightarrow Z^0H^0,\ Z^0 \rightarrow e^+e^- \text{ or } \mu^+\mu^-,\ H^0 \rightarrow \mathit{undetected}$$

$$e^+e^- \rightarrow Z^0H^0,\ Z^0 \rightarrow \nu\bar{\nu},\ H^0 \rightarrow e^+e^- \text{ or } \gamma\gamma$$

where the Z^0 can either be real or virtual depending on the beam energy.

In these processes the Z^0 and H^0 recoil against each other with an average momentum of approximately 9 GeV/c for a centre-of-mass energy of 91 GeV. In the first reaction the decay products of the Z^0 are boosted away from the undetected Higgs. The limit on this reaction was obtained by searching for events in which the two observed leptons were acollinear in the plane perpendicular to the beam direction (acoplanar). A characteristic signature of the second reaction is the presence of isolated electromagnetic energy deposition. The limit on both visible decay channels of the low-mass Higgs was determined by searching for events having all electromagnetic energy confined to a 30° half-angle cone and no other activity in the detector. Searches for $H^0 \rightarrow$ *undetected* and $H^0 \rightarrow e^+e^-$ at LEP have been recently reported by the ALEPH collaboration [17]. Apart from the search described here, no LEP experiment has reported on a direct search for the process $H^0 \rightarrow \gamma\gamma$.

2 The OPAL detector

The data were recorded at the CERN e^+e^- collider LEP during its Fall 1989 run and correspond to an integrated luminosity of about 1.2 pb^{-1}. The measurements reported here made use of the OPAL detector [18], which is a multipurpose apparatus having nearly 4π steradian acceptance. The central detector (CD) consists of a system of tracking chambers inside a 0.435 Tesla solenoidal magnetic field. The CD system is surrounded by a time-of-flight (TOF) counter array, a lead glass electromagnetic calorimeter (EC) with a presampler, an instrumented magnet return yoke serving as a hadron calorimeter (HC), four layers of outer muon chambers (MU), and an endcap system that includes a low-angle forward detector (FD). The analysis presented here relies mostly on the EC, CD, and FD systems. Cosmic ray rejection made use of the TOF, HC and MU systems.

The central tracking detector consists of an inner precision vertex chamber, a large volume 'jet' chamber and outer chambers for tracking in the direction along the beam. The coordinate system is defined with z along the beam axis, and θ and ϕ the polar and azimuthal angles. The main tracking is performed using the jet chamber. This is a drift chamber segmented into 24 ϕ sectors with 159 radial layers of sense-wires and is approximately four metres in length and two metres in radius. The region of tracking registering a minimum of 40 wires covers approximately $|\cos\theta| \leq 0.94$. The TOF system is located outside the magnet coil and covers the barrel region of $|\cos\theta| \leq 0.82$. It has 160 scintillator bars, 6.8 m long and 45 mm thick, located at a radius of 2.4 m. The presampler for the barrel electromagnetic calorimeter surrounds the TOF system and consists of 2 layers of limited streamer mode tubes. The electromagnetic calorimeter consists of a cylindrical array of 9,440 lead glass blocks of 24.6 radiation lengths thickness in the barrel region, covering the range $|\cos\theta| < 0.82$, and 2,264 lead glass blocks of 20 radiation lengths thickness in the endcaps, covering the range $0.81 < |\cos\theta| < 0.98$. Each block subtends a solid angle of approximately 40×40 $mrad^2$. The blocks project towards a point near the interaction point in the barrel region, and along the beam direction in the endcaps. The electromagnetic calorimeter covers 98% of the solid angle.

The luminosity of the colliding beams was determined by observing small angle Bhabha scattering with the forward detector [19], a lead/scintillator calorimeter with associated tracking chambers, at either end of the central detector, with an acceptance from 40 to 150 mrad in polar angle (θ) and 2π in azimuth. The Bhabha cross section used for normalization is approximately 45 nb.

3 The Monte Carlo Generators

To study the process $e^+e^- \rightarrow H^0Z^0$ the decays were modelled using a generator based on the Berends and Kleiss formalism [20] for $e^+e^- \rightarrow H^0\mu^+\mu^-$, where initial state radiation is taken into account to first order. The cross section was calculated using the Improved Born Approximation [21] incorporating the value of $m_Z = 91.15$ GeV/c^2 [19] with the corresponding Standard Model value for Γ_Z, and taking into account the effective electroweak couplings $\alpha(Q^2)$ and $\sin^2\theta_W$ [22] at the Z^0 mass. A more rigorous treatment of initial state radiative corrections via exponentiation was then applied using the formalism described in reference [23]. The theoretical uncertainty on the cross section obtained in this manner is estimated to be better than $\pm 2\%$. This is based on studying the sensitivity of the cross section to the Z^0 mass and top quark mass after including the contribution of the top quark triangle graph at the ZHZ vertex described in reference [24].

The momentum spectrum of the low-mass Higgs boson is sensitive to the centre-of-mass energy

and to initial state radiation. The signal acceptance is sensitive to the Higgs momentum (p_H) because the probability for the Higgs boson to decay outside the detector depends on the mean decay length which is equal to $\frac{p_H}{m_H}c\tau$. In the case of the $Z^0 \rightarrow \nu\bar{\nu}$ search channel, an additional dependence on the spectrum is introduced by the requirement that a minimum energy be deposited in EC by the decay products of the Higgs boson in order to trigger the experiment. It has been estimated that the omission of higher order initial state radiation introduced a 1% uncertainty in the calculation of the acceptance. The dependence on centre-of-mass energy was accounted for by calculating the number of H^0 events expected in the data as a function of E_{cm} using the Monte Carlo described above.

H^0 events were generated for different values of m_H, assuming the lowest order Standard Model width of the Higgs boson for $2m_e < m_H < 2m_\mu$:

$$\Gamma_H = \frac{G_F m_e^2 m_H}{4\pi\sqrt{2}}(1 - 4m_e^2/m_H^2)^{\frac{3}{2}}.$$

Since the momentum spectrum of the Higgs boson is almost independent of the Higgs boson mass for the range of masses considered here, the mean decay length of the Higgs boson is inversely proportional to the square of the mass.

The OPAL detector response to the generated particles was modelled using a Monte Carlo program [25] based on the GEANT [26] package, which provides a detailed description of the response of the various detector components to annihilation events.

4 Search for $Z^0 \rightarrow e^+e^-H^0$ or $\mu^+\mu^-H^0$, $(H^0 \rightarrow \mathit{undetected})$

Electron and muon pairs were identified on the basis of the two highest momentum CD tracks with opposite sign. These tracks are referred to as the primary tracks. For this study, CD tracks were required to have at least 40 hits, to have a distance of closest approach to the origin in the plane perpendicular to the beam of less than 2.5 cm and in the coordinate along the beam of less than 50 cm, and to be associated to an EC cluster with an energy of at least 250 MeV. In addition, each primary track was required to have a momentum of at least 5 GeV/c and $|\cos\theta| < 0.9$. An initial cut required that there be no track outside cones of half-angle 15° centred about each of the primary tracks and that the missing momentum vector of the event, as computed from the momentum vectors of the primary tracks, have $|\cos\theta| < 0.9$. The background from two photon events was reduced by requiring that less than 2 GeV be deposited in the forward detector and that the angle between the two tracks be greater than 90°.

After applying these cuts a sample of 2861 events, predominantly lepton pairs, remained. The process $Z^0 \rightarrow l^+l^-H^0$; $H^0 \rightarrow$ *undetected* was distinguished from $Z^0 \rightarrow l^+l^-$ on the basis of acoplanarity and the momenta of the primary tracks. The acoplanarity angle, ϕ_{acop}, is the supplement of the azimuthal angle between two momentum vectors. Each momentum vector used to calculate ϕ_{acop} was formed by vectorially summing the momentum of the primary track, electromagnetic energy associated to the primary track which was in excess of the momentum of the primary track, and any unassociated electromagnetic energy inside a 5° cone about the primary track. Cuts were placed on the weighted acoplanarity given by

$$\alpha = \phi_{acop} < \sin\theta >$$

where $< \sin\theta >$ is the average of the absolute values of the sine of the polar angles of the EC clusters associated to the primary tracks. The weighted acoplanarity has the desirable quality

that it is related to the minimum energy of a photon radiated from an e^+e^- or $\mu^+\mu^-$ pair by $E_{min} \simeq \alpha E_{beam}$.

Dilepton Z^0 decays can give rise to final states with acoplanar tracks due the presence of initial and final state radiation, and, in the case of τ pairs, due to the missing energy carried away by neutrinos. Background due to radiative photons was eliminated by requiring that the sum of all electromagnetic energy outside of two cones of half-angle 5° about the primary tracks be less than 1 GeV, which is well above the level of detector noise. The decay of τ pairs can result in final states with acoplanarity of more than about 50 mrad only if one or more of the neutrinos has a large momentum. This background can be reduced without significantly reducing the acceptance to the Higgs boson signal by placing cuts on the momentum of the more energetic primary track, p_1, and on the momentum of the less energetic primary track, p_2. For muon pairs this momentum measurement was made using CD tracks. For electrons two measurements were available. The energy resolution of the electromagnetic calorimeter was in general better than that of the tracking, except on the boundary region between the endcap and barrel electromagnetic calorimeters. To maintain a high acceptance in all regions of the detector, p_1 and p_2 were calculated using both tracks and electromagnetic clusters, and the larger of the two was used. Figure 1-a shows the distribution of p_2 versus α for the two primary tracks from a sample of Monte Carlo τ pair events equivalent to approximately 4.5 times the number of τ pairs produced in the data sample considered here. The generator described in reference [27] was used to describe the $Z^0 \rightarrow \tau^+\tau^-$ background. Based on a comparison of the expected distribution for the Higgs boson signal (Figure 1-b) and the τ pair Monte Carlo, the following cuts were placed on weighted acoplanarity and primary track momenta:

- $\alpha > \alpha_0$ where $\alpha_0 = 35$ mrad
- $p_1 > 40 - 100(\alpha - \alpha_0)$ GeV/c
- $p_2 > 30 - 200(\alpha - \alpha_0)$ GeV/c
- $p_1, p_2 > 10$ GeV/c.

The minimum value of weighted acoplanarity, 35 mrad, corresponds to a minimum momentum for radiative photons of about 1.6 GeV/c, which is well matched to the 1 GeV cut on electromagnetic energy outside of the 5° cones around the primary tracks. The cut on p_1 removed τ pairs where both visible tracks had almost the same momenta. This had little effect on the acceptance for the Higgs boson. Figure 1-c shows the p_2 versus weighted acoplanarity for the data. After applying the weighted acoplanarity and momentum cuts to the data no events remained.

At the Z^0 peak the signal acceptance, as determined from the Monte Carlo, is 42% for electron pairs and 41% for muon pairs produced in association with a Higgs boson decaying outside of the detector. The major loss in acceptance comes from those Higgs events associated with muon and electron pairs of very small acoplanarity. Corrections to this acceptance were necessary to account for inadequacies of the Monte Carlo simulation when describing the effects of the p_1 and p_2 cuts. These corrections were obtained by applying the cuts to data containing well identified e^+e^- or $\mu^+\mu^-$ decays of the Z^0. A correction of 0.82 was required for muon pairs which accounts for the difference between the momentum resolution in the data and that used in the Monte Carlo and some effects of the lack of final state radiation in the Higgs generator. For electrons this factor was 0.96 owing to the more accurate simulation of the electromagnetic calorimeters in the Monte Carlo.

A correction was also applied to allow for the lack of final state radiation in the event generator. A lower bound on this correction was obtained from a study of well identified electron and muon decays of the Z^0 taken at centre-of-mass energies within 1 GeV of M_Z. For the e^+e^- pairs the

total electromagnetic energy was required to exceed 80% of the centre-of-mass energy and the polar angle of the electron was required to satisfy $-0.9 < \cos\theta < 0.5$ in order to select s-channel events. The fraction of electron pairs with less than 1 GeV of electromagnetic energy outside of the two 5° cones around the primary tracks was found to be 0.83. For muon pairs selected as in reference [28], this factor was 0.88.

The resolution of the weighted acoplanarity was determined using $\mu^+\mu^-$ and e^+e^- events in the data and compared to that predicted by Monte Carlo [27,29]. The difference between data and Monte Carlo resolutions is less than 0.2 mrad. This difference introduces a negligible effect on the determination of signal acceptance.

The trigger efficiency for electrons was determined from redundant triggers to be 100% when both endcap and barrel electromagnetic triggers were active. After accounting for inefficiencies associated with inactive triggers the overall efficiency was 98%. For muons, only triggers in the barrel region ($|\cos\theta| < 0.82$) were considered. In the barrel region the trigger efficiency was better than 99% for tracks with an acoplanarity smaller than 250 mrad, falling to 96% for highly acoplanar events. Taking into account periods during which not all triggers were active, the muon trigger efficiency was 98%. After all cuts, the overall trigger efficiency including geometrical acceptance was 84%.

Combining the corrected Monte Carlo efficiency with the trigger efficiencies and the correction for final state radiation, the overall efficiencies for detecting lepton pairs produced in association with long lived Higgs bosons were 33% for electron pairs and 25% for muon pairs. These efficiencies are summarized in Table 1. The dependence of the acceptance on the Higgs boson lifetime was determined using a Monte Carlo calculation, the results of which are tabulated in Table 2. The expected number of Higgs bosons can be calculated from luminosities and cross sections given in Table 3 and the overall efficiency as a function of Higgs boson mass from Table 1. Using 3.4% for the branching ratio of the Z^0 to electrons and muons, 6.1 events are expected if all Higgs bosons decay outside the detector.

The limit on the Higgs boson mass from this search was set conservatively by subtracting one standard deviation in the systematic error from the predicted number of expected events at each mass. The mass limit is set where the expected number drops below 3 events, which is the Poisson 95% confidence level if no candidate events are observed [30]. The systematic error includes contributions from the errors due to (a) the Monte Carlo detector simulation (5%), (b) Monte Carlo statistics (5%), (c) treatment of initial state radiation (1%), (d) theoretical cross section (2%), and (e) luminosity and overall normalization (4%). Adding these effects in quadrature, a total of 10% is obtained. Figure 4 shows the variation in the number of expected events, less the systematic error, as function of Higgs boson mass, assuming the Standard Model prediction for the Higgs boson lifetime. Using only this search, a Standard Model Higgs boson with a mass less than 40 MeV/c^2 is excluded at the 95% confidence level.

5 Search for $Z^0 \to \nu\bar{\nu}H^0, (H^0 \to e^+e^-)$ or $(H^0 \to \gamma\gamma)$

Higgs bosons decaying to e^+e^- or $\gamma\gamma$ before or within the electromagnetic calorimeter will produce isolated electromagnetic clusters when the Z^0 decays to $\nu\bar{\nu}$. The distribution of the expected electromagnetic energy deposited in the barrel calorimeter for a Higgs boson with mass 100 MeV/c^2 and decaying to e^+e^- is shown in Figure 2. $H^0 \to e^+e^-$ or $\gamma\gamma$ events would have triggered the detector if either (a) a minimum of 4 GeV was deposited in the barrel EC and at least one charged

particle was detected by the TOF system or (b) the pair deposited at least 6 GeV in the barrel EC. The efficiency of trigger (a) is plotted as a function of the barrel EC energy in Figure 2. Photons produced in the $H^0 \to \gamma\gamma$ channel have a high conversion rate in the material located before the TOF and therefore trigger (a) is only 2% less efficient for the $H^0 \to \gamma\gamma$ channel than for the $H^0 \to e^+e^-$ channel. For simplicity, this inefficiency has been included in all subsequent considerations of the trigger efficiency.

Efficiencies of the barrel EC triggers were measured using all data which were accepted by non-EC trigger elements of the detector. The TOF trigger efficiency was measured to be 0.981 ± 0.007 using radiative Bhabha events that produced single electrons at large angles to the beam and which also deposited enough energy in the forward detector to independently trigger the experiment. The energy spectrum of these electrons is well matched to that of the Higgs boson decay. An online selection of events was performed by a filter algorithm that selected events having a total EC energy in excess of 4 GeV with a TOF measurement occurring no more than 27 ns after the beam crossing. The efficiency of this filter was also checked using these events. Agreement was found between measured and simulated filter efficiencies both as a function of energy deposition and polar angle.

A high selection efficiency for $H^0 \to e^+e^-$ or $\gamma\gamma$, $Z^0 \to \nu\bar{\nu}$ passing the trigger and filter requirements was obtained by demanding that at least 4 GeV be deposited within a 30° half-angle cone about the largest electromagnetic cluster and that the EC energy outside the 30° cone be less than 0.5 GeV. The cone axis was required to be oriented with $|\cos\theta| < 0.75$. The effects of noise were minimized by using only those EC clusters in the barrel that had at least 170 MeV and those clusters in the endcap that had at least 250 MeV and contained at least two lead glass blocks. $Z^0 \to l^+l^-$ and $Z^0 \to q\bar{q}$ events were removed by further demanding that no track intersect the electromagnetic calorimeter outside this cone and that there be less than ten tracks in the event. All tracks used to veto events in this analysis had to have at least 30 hits. The backgrounds from two photon and radiative Bhabha events were removed by rejecting events with more than 2 GeV deposited in the forward detector.

The remaining events, after the above requirements, were due to cosmic ray muons and beam halo particles. These backgrounds were eliminated by rejecting any event which satisfied one of the following criteria:

- A muon chamber track was present.
- The barrel hadron calorimeter recorded more than 4 GeV energy deposition.
- More than 3 of the 8 outer layers of the hadron calorimeter registered strip hits within a 45° road in the r-ϕ plane.
- Electromagnetic clusters had a width in ϕ or θ greater than 0.25 mrad were present.
- A TOF measurement was more than 10 ns from the expected flight time for Higgs events. (If no TOF measurement was present but a large presampler signal was registered then the event was assumed to have occurred outside the timing window required to making a TOF measurement.)
- Two TOF measurements had a time difference of more than 2 ns, were consistent (within 2 ns) with a single cosmic ray, and were inconsistent (greater than 2 ns) with two particles coming from the interaction point.
- Tracks were present whose innermost point, as determined from a track fit, was more than 150 cm from the interaction region along the beam.

One event passed all cuts, consistent with the 1.8 ± 0.2 expected background events from $e^+e^- \rightarrow \nu\bar{\nu}\gamma$, as estimated using the Monte Carlo generator described in reference [31]. The surviving event contained no evidence of a track, the energy of the largest EC cluster was 4.8 GeV and the centre-of-mass energy was 91.5 GeV.

Apart from the energy deposition in the forward detector, the Higgs boson signature in the EC that is used in this analysis is similar to that of wide angle single electron and single photon events from radiative Bhabha scattering [32]. A check of the selection process was provided by measuring the number of such events that survive the same trigger and filter requirements and all cuts but the forward detector cut. After applying all cuts except the forward detector cut, and further demanding that the forward detector energy be greater than 30 GeV and that one track be found, 45 single electron events remained. Using the Monte Carlo generator described in reference [32] the number of expected events was found to be 49 ± 6 (stat)±4 (sys), in good agreement with the number observed. The distribution of the EC energy of these electrons is presented in Figure 3. The good agreement between data and Monte Carlo EC energy distributions provides evidence that the response of the detector to the decay products of the Higgs has been reliably simulated. A similar check was performed with radiative Bhabha events in which a photon is directed into the barrel. As before, the forward detector energy was required to be greater than 30 GeV. From the Monte Carlo, 4.7 ± 0.8 (stat) ±0.4 (sys) events were predicted, and 3 events were observed. Again, there is agreement between predicted and observed rates. Although statistics are limited, these cross checks confirm that the OPAL detector is sensitive to $H^0 \rightarrow e^+e^-$ and $H^0 \rightarrow \gamma\gamma$ events.

Some loss of signal efficiency arises from the presence of noise in the calorimeters because of the requirement that the electromagnetic energy outside the 30° cone be less than 0.5 GeV. This loss of efficiency was evaluated by measuring the total electromagnetic calorimeter energy in random beam crossing events and by using collinear Bhabha events restricted to $|\cos\theta| < 0.75$. Based on these studies an efficiency of $98.1 \pm 0.6 \pm^{0.5}_{0.9}\%$ was assigned to the effects of EC noise arising through this cut. Similar studies, employing data, were used to measure the efficiencies of the forward detector cut ($99.9 \pm 0.1\%$), muon cut ($99.9 \pm 0.1\%$), barrel hadron calorimeter cut ($98.7 \pm 0.6\%$), hadron strip veto cut ($99.7 \pm 0.3\%$) and the TOF requirements (99.8%). The combined efficiency arising from these various measured detector effects is ($96.1 \pm 1.3\%$).

Table 2 shows the mean lifetime, overall selection efficiency after applying all cuts, and the number of Standard Model Higgs bosons expected to be detected using this analysis for masses varying between 10 and 200 MeV/c^2. Because of the sensitivity of this analysis to trigger thresholds and detector performance, some data which were used in the search for ($H^0 \rightarrow$ *undetected*) were excluded for this analysis, reducing the expected number of events by 16%. Using the Standard Model branching ratio of $Z^0 \rightarrow \nu\bar{\nu}$ of 0.20, the expected number of events is 17 for Higgs bosons which decay inside the detector. The various contributions to the systematic error on the efficiencies are: (a) simulation of the electromagnetic calorimeter (5.3%), (b) trigger simulation (2.8%) (c) filter simulation (5.1%), (d) Monte Carlo statistics (7%), (e) error on the efficiencies of noise related cut (1.3%) (f) treatment of initial state radiation (1%), (g) theoretical cross section (2%) and (h) luminosity and overall normalization (4%) leading to a total systematic error of 12%. Figure 4 shows the number of events, as predicted by the Standard Model, as a function of Higgs boson mass for $H^0 \rightarrow e^+e^-$. Since one event, consistent with a background of 1.8, has been observed, the 95% confidence level is reached at 3.8 events. A Standard Model Higgs boson with a mass in the range of 30 MeV/c^2 to $2m_\mu$ is ruled out at the 95% confidence level on the basis of this analysis alone.

6 Combined Mass Limits

The number of observable H^0 events predicted by the Standard Model in each of the two channels, $H^0 \rightarrow$ *undetected* and $H^0 \rightarrow e^+e^-$ or $\gamma\gamma$, as a function of m_H, is shown in Figure 4. Also shown in the figure are the upper limits for observing a signal at the 95% confidence level which depends on the expected number of events in each of the two channels and varies from 3 events at zero mass to 3.8 events at $2m_\mu$ using the procedure described in reference [30]. The confidence intervals were estimated by reducing the predicted signal (sum of both channels) by one standard deviation in the systematic error. The combined searches for $H^0 \rightarrow$ *undetected* and $H^0 \rightarrow e^+e^-$ or $\gamma\gamma$ exclude a minimal Standard Model Higgs boson having a mass in the range $0 \leq m_H \leq 2m_\mu$ at *at least* the 95% confidence level in agreement with reference [17]. Since the two analyses cover all lifetimes and decay products of the Higgs boson below the $2m_\mu$ threshold, they exclude the existence of all nonstandard Higgs bosons whose production rate is at least that of the Standard Model. The 95% confidence level for nonstandard Higgs bosons whose coupling is reduced with respect to the Standard Model is determined by the ratio of the number of events needed for the 95% confidence level and the total number events expected for the Standard Model. Thus all nonstandard Higgs bosons whose rate in the process $e^+e^- \rightarrow H^0Z^0$ is at least 57% that of the Standard Model Higgs boson are excluded at the 95% confidence level.

Acknowledgements

It is a pleasure to thank the SL Division for the efficient operation of the LEP accelerator, the precise information on the absolute energy, and their continuing close cooperation with our experimental group. The assistance of W. Hollik in understanding the Higgs production cross section calculation is also gratefully acknowledged. In addition to the support staff at our own institutions we are pleased to acknowledge the following :
Department of Energy, USA
National Science Foundation, USA
Science and Engineering Research Council, UK
Natural Sciences and Engineering Research Council,Canada
Israeli Ministry of Science
Minerva Gesellschaft
The Japanese Ministry of Education, Science and Culture (the Monbusho) and a grant under the Monbusho International Science Research Program
American Israeli Bi-national Science Foundation
Direction des Sciences de la Matiere, France
The Bundesministerium für Forschung und Technologie, FRG
and The A.P. Sloan Foundation.

References

[1] S. L. Glashow, J. Iliopoulos and L. Maiani, Phys. Rev. **D2** (1970) 1285 ; S. Weinberg, Phys. Rev. Lett. **19** (1967) 1264; A. Salam, *Elementary Particle Theory*, ed. N. Svartholm (Almquist and Wiksells, Stockholm, 1969), p. 367.

[2] P. W. Higgs, Phys. Lett. **12** (1964) 132; F. Englert and R. Brout, Phys. Rev. Lett. **13** (1964) 321; G. S. Guralnik, C. R. Hagen, and T. W. B. Kibble, Phys. Rev. Lett. **13** (1964) 585.

[3] S. Coleman and E. Weinberg, Phys. Rev. **D7** (1973) 1888; A. D. Linde, JETP Lett. **23** (1976) 64; A. D. Linde, Phys. Lett. **B70** (1977) 306; S. Weinberg, Phys. Rev. Lett. **36** (1976) 294.

[4] M. Lindner, M. Sher and H. W. Zaglauer, FERMILAB-PUB-88/206-T (1988); H. D. Politzer and S. Wolfram, Phys. Lett. **B82** (1978) 242 and (E) **83B** (1979) 421; E. Gross and E. Duchovni, Phys. Rev. **D38** (1988) 2308.

[5] I. Beltrami *et al.*, Nucl. Phys. **A451** (1986) 679.

[6] D. Kohler *et al.*, Phys. Rev. Lett. **33** (1974) 1628.

[7] S.J. Freedman *et al.*, Phys. Rev. Lett. **52** (1984) 240.

[8] R. Barbieri and T.E.O. Ericson, Phys. Lett. **B57** (1975) 270.

[9] Reviews of the experimental searches can be found in: P. J. Franzini and P. Taxil (conveners), *Higgs Search* in CERN 89-08, v. 2, p. 59 (1989); S. Dawson, J. F. Gunion, H. E. Haber and G. L. Kane, *The Higgs Hunter's Guide*, BNL-41644 (1989), submitted to Phys. Rep..

[10] G.D.Barr *et al.*, Phys. Lett. **B235** (1990) 356.

[11] Y. Asanao *et al.*, Phys. Lett. **B113** (1982) 195.

[12] S. Egli *et al.*, SINDRUM Collab., Phys. Lett. **B222** (1989) 533.

[13] S. Raby, G. B. West and C.M. Hoffman, Phys. Rev. **D38** (1989) 828. H.E. Haber, Santa Cruz preprint SCIPP 89/43 (1989).

[14] S. Dawson, Phys. Lett **B222** (1989) 143.

[15] M. Davier and H. Nguyen Ngoc, Phys. Lett. **B229** (1989) 150.

[16] J. Ellis, M. K. Gaillard and D. V. Nanopoulos, Nucl. Phys. **B106** (1976) 292;
P. J. Franzini and P. Taxil (conveners), *Higgs Search* in CERN 89-08, v. 2, p. 59 (1989).

[17] D. Decamp *et al.*, ALEPH Collab., Phys. Lett. **B236** (1990) 233; D. Decamp *et al*, ALEPH Collab., Phys. Lett. **B245** (1990) 289.

[18] K. Ahmet *et al.*, OPAL Collab., *The OPAL Detector at LEP*, (to be sumbitted to Nucl. Instr. and Meth.).

[19] M. Z. Akrawy *et al.*, OPAL Collab., **B240**(1990)497.

[20] F. A. Berends and R. Kleiss, Nucl. Phys. **B260** (1985) 32.

[21] R. L. Kelly and T. Shimada, Phys. Rev. **D23** (1981) 1940; J. Ellis and R. Peccei, editors, *Physics at LEP*, CERN 86-02, v. 1 (1986); reference [20].

[22] M. Consoli *et al.*, *Electroweak Radiative Corrections for Z Physics*, in CERN 89-08, v. 2 (1989), eds. G. Altarelli, R. Kleiss and C. Verzegnassi; D. C. Kennedy and B. W. Lynn, Nucl. Phys. **B322** (1989) 1; W. Hollik, private communication.

[23] G. Burgers, *Shape and Size of the Z Resonance in Polarization at LEP*, in CERN 88-06 (G. Alexander, G. Altarelli, A. Blondel and C. Coignet, eds.) (1988).

[24] Z. Hioki, Phys. Lett. **B224** (1989) 417.

[25] J.Allison *et al.*, Computer Physics Communications **47** (1987) 55.

[26] R. Brun, F. Bruyant, M. Maire, A. C. McPherson and P. Zanarini, *GEANT3*, CERN DD/EE/84-1 (1987).

[27] S. Jadach, B. F. L. Ward, Z. Was, R. G. S. Stuart, and W. Hollik, *KORALZ the Monte Carlo Program for τ and μ pair Production Processes at LEP/SLC*, unpublished (1989).

[28] M. Z. Akrawy *et al.*, OPAL Collab., **B235**(1990)379.

[29] M. Böhm,A.Denner and W.Hollik, Nucl. Phys. **B304**(1988)687,
F.A.Berends, R.Kleiss, W.Hollik, Nucl. Phys. **B304**(1988)712.

[30] G.P. Yost *et al.*, Particle Data Group, Phys. Lett. **B204**(1988) 81;
O. Helene, Nucl. Instr. and Meth., **B212**(1983)319.

[31] F.A.Berends, G.J.H.Burgers, C. Mana, M. Martinez and W.L. van Neerven, Nucl. Phys. **B301** (1988) 583.

[32] D. Karlen, Nucl. Phys. **B289** (1987) 23.

Tables

Table 1: The contributions to the overall efficiency for $H^0 \rightarrow$ *undetected* produced in association with electron and muon pairs.

	Uncorrected Monte Carlo	Correction to Monte Carlo Momentum	Trigger Efficiency	Correction for Radiation	Overall Efficiency
electrons	0.42	0.96	0.98	0.83	0.33
muons	0.41	0.82	0.84	0.88	0.25

Table 2: The mean lifetime, overall selection efficiency and the number of Higgs bosons predicted in the minimal Standard Model as a function of the Higgs boson mass assuming a 100% decay branching ratio in each channel. (Note that due to the large boost of the light Higgs bosons the decay path can be much longer than $c\tau$.)

Higgs Mass (MeV/c^2)	$c\tau$ (cm)	Detection Efficiency (%)		Number of Predicted Events	
		$H^0 \rightarrow$ *undetected*	$H^0 \rightarrow e^+e^-, \gamma\gamma$	$H^0 \rightarrow$ *undetected*	$H^0 \rightarrow e^+e^-, \gamma\gamma$
5	24.6	29	-	6.1	-
10	11.7	28	1	5.8	0.4
20	5.8	25	3	5.3	1.6
30	3.8	21	7	4.4	3.4
40	2.9	17	11	3.6	5.5
50	2.3	13	15	2.7	7.6
100	1.2	1	28	0.2	14.4
150	0.8	-	32	-	16.5
200	0.6	-	33	-	17.0

Table 3: Cross section of $e^+e^- \rightarrow H^0Z^0$ for a 30 MeV Higgs boson and integrated luminosities for the data as a function of centre-of-mass energy. ϵ_{rel} is the efficiency relative to the peak for the selection procedures. The luminosities are calculated for data collected with the CD at operating voltage and both endcap and barrel electromagnetic calorimeters functioning properly. The overall systematic error is 30 MeV on the energy scale and 4% on the luminosity and normalization.

Centre-of-Mass Energy (GeV)	Cross section for $e^+e^- \rightarrow Z^0H^0$ (nb)	Luminosity $\int \mathcal{L}dt$ (nb^{-1})	Relative Efficiency	
			$H^0 \rightarrow e^+e^-$ or $\gamma\gamma$	$H^0 \rightarrow$ *undetected*
			ϵ_{rel}	ϵ_{rel}
88.28	0.026	124	1.18	1.31
89.29	0.062	67	1.13	1.31
90.28	0.179	107	1.06	1.06
91.03	0.354	195	1.00	1.00
91.29	0.398	214	0.93	0.93
91.53	0.418	183	0.87	0.87
92.31	0.370	89	0.75	0.76
93.28	0.268	104	0.70	0.76
94.28	0.202	92	0.78	0.79
95.04	0.169	18	0.93	0.83

Figures

Figure 1: (a) p_2 versus weighted acoplanarity for a Monte Carlo simulation of τ pair events. This represents approximately 4.5 times the number of τ pairs produced in the data. (b) p_2 versus weighted acoplanarity for a Monte Carlo simulation of 2 MeV/c^2 Higgs bosons produced in association with muon pairs. The region above the curve is the signal region and was chosen on the basis of the τ Monte Carlo. (c) p_2 versus weighted acoplanarity after all other cuts for the data.

Figure 2: Monte Carlo distribution of the energy deposited in the barrel EC for a 100 MeV/c^2 mass Higgs boson decaying to e^+e^-. Superimposed is the measured efficiency of the trigger requiring barrel EC and TOF as a function of the barrel EC energy.

Figure 3: Energy spectrum of single electrons having $|\cos\theta| < 0.75$ produced in radiative Bhabha events passing all cuts described in Section 5 with the exceptions that there be at least 30 GeV deposited in the forward detector and that the event contain one charged track. The points are the OPAL data while the histogram represents Monte Carlo generated events.

Figure 4: Predicted number of detected H^0 events in the OPAL detector *vs* the Higgs boson mass. $H^0 \rightarrow e^+e^-$ or $\gamma\gamma$ and $H^0 \rightarrow$ *undetected* are shown both separately and combined. The predicted number of events for both channels has been reduced by one standard deviation in the systematic error. The 95% confidence level takes into account the observation of one event, consistent with background, in the channel $H^0 \rightarrow e^+e^-$ or $\gamma\gamma$.

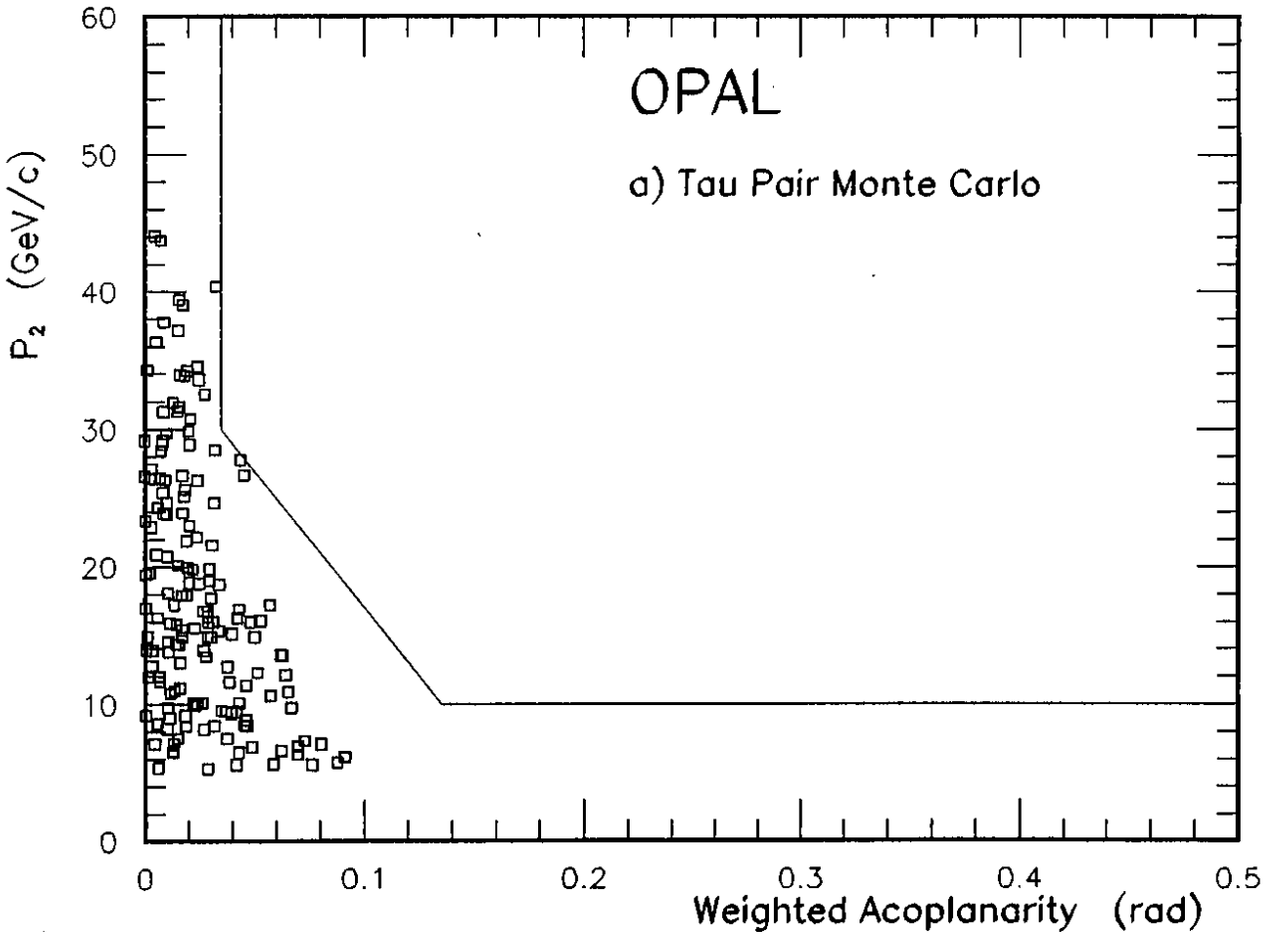
OPAL
a) Tau Pair Monte Carlo
P_2 (GeV/c)
60
50
40
30
20
10
0
0
0.1
0.2
0.3
0.4
0.5
Weighted Acoplanarity (rad)

FIGURE 1–a

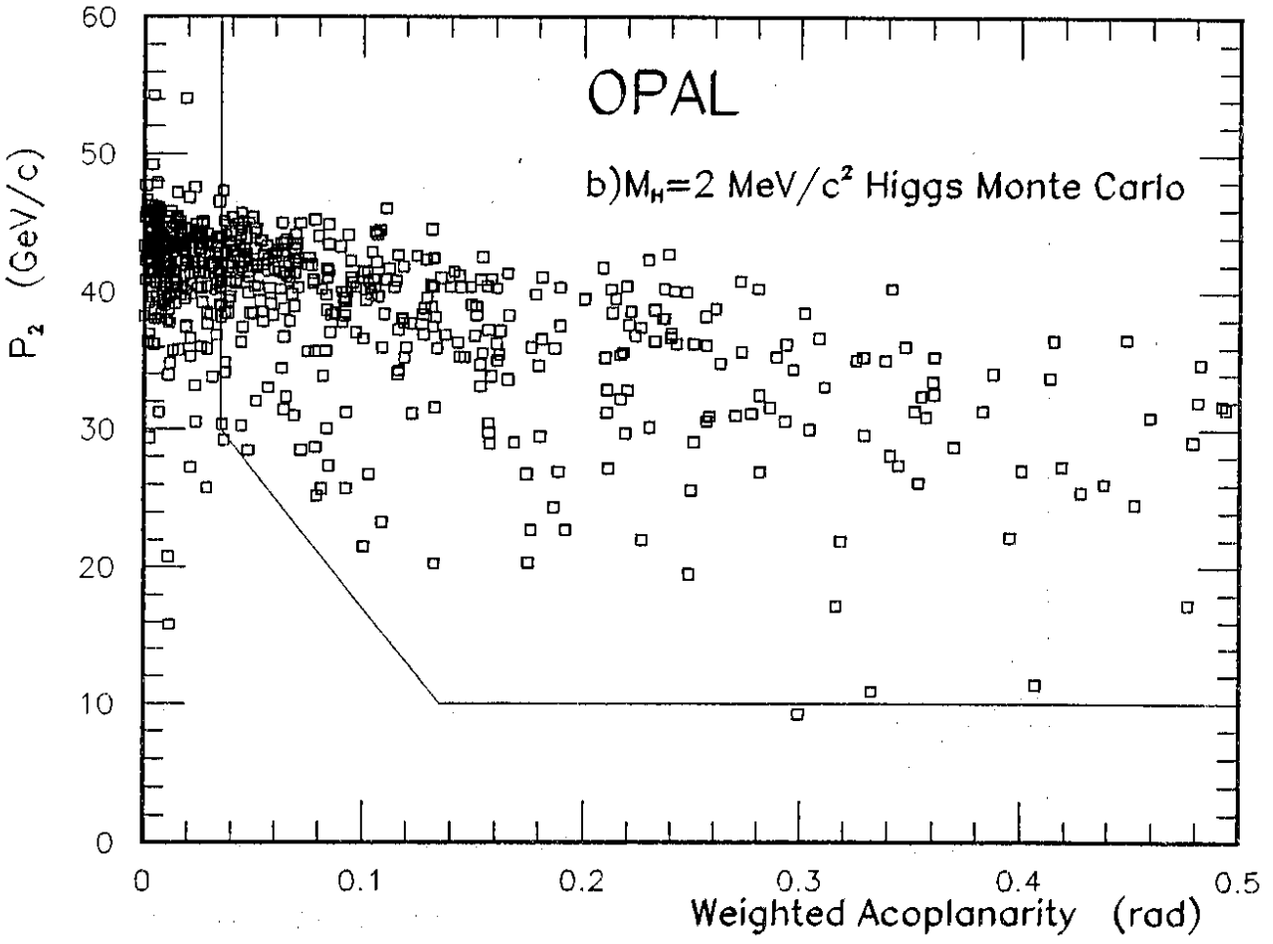
OPAL
b)M_H=2 MeV/c^2 Higgs Monte Carlo
P_2 (GeV/c)
Weighted Acoplanarity (rad)
0
10
20
30
40
50
60
0
0.1
0.2
0.3
0.4
0.5

FIGURE 1–b

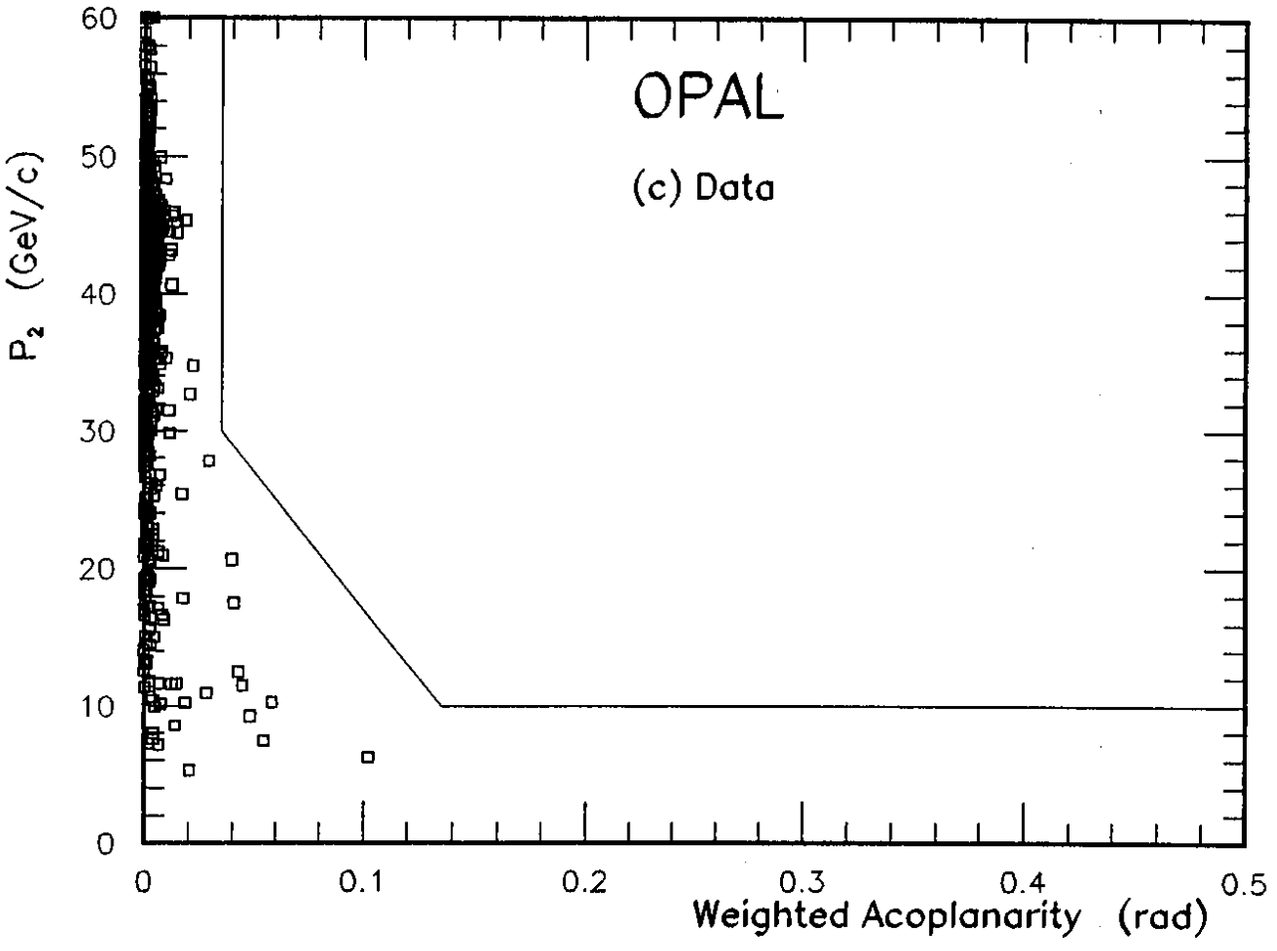
OPAL
(c) Data
P_2 (GeV/c)
Weighted Acoplanarity (rad)
0
10
20
30
40
50
60
0
0.1
0.2
0.3
0.4
0.5

FIGURE 1–c

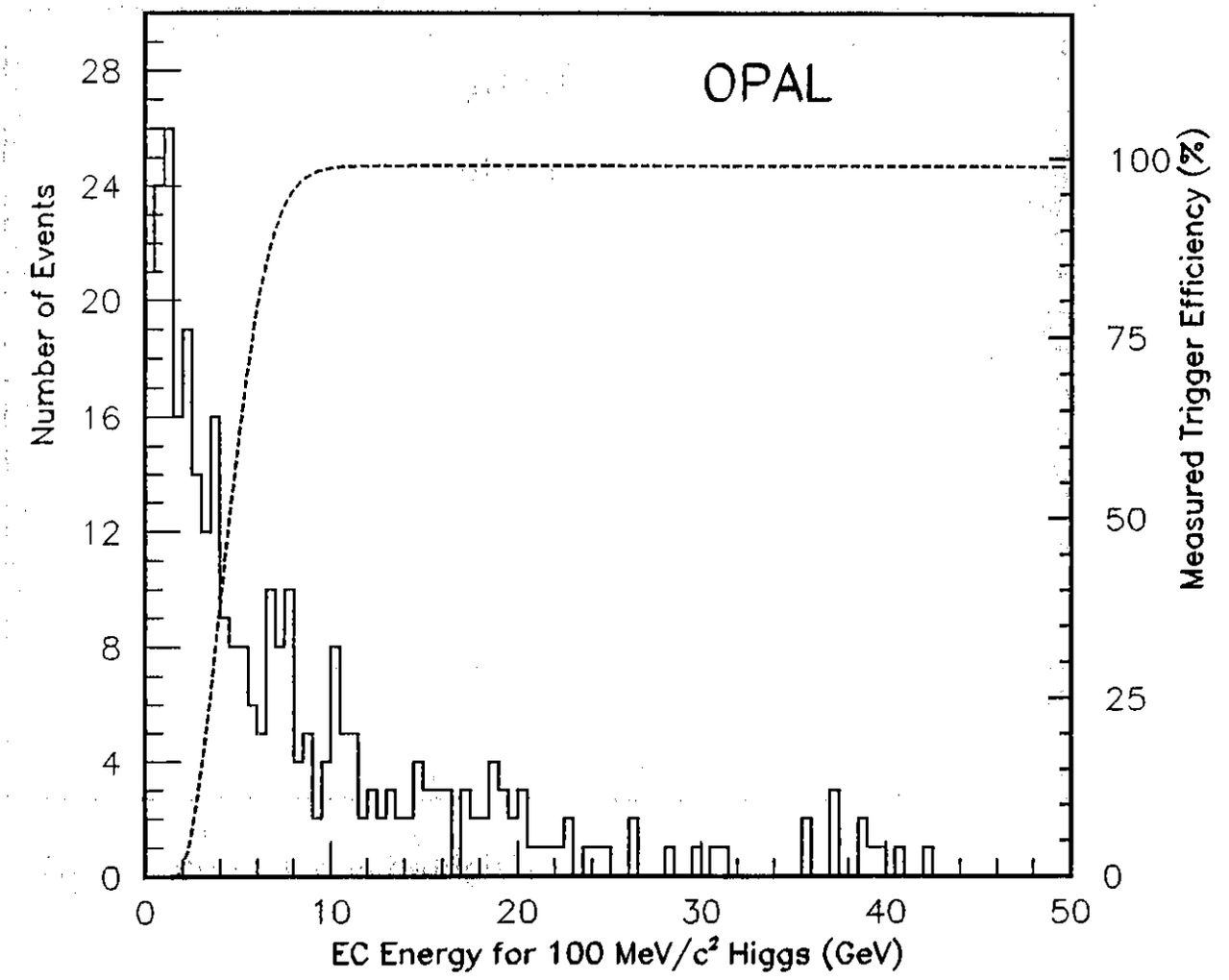
OPAL
Number of Events
Measured Trigger Efficiency (%)
EC Energy for 100 MeV/c² Higgs (GeV)
0
4
8
12
16
20
24
28
0
25
50
75
100
0
10
20
30
40
50

FIGURE 2

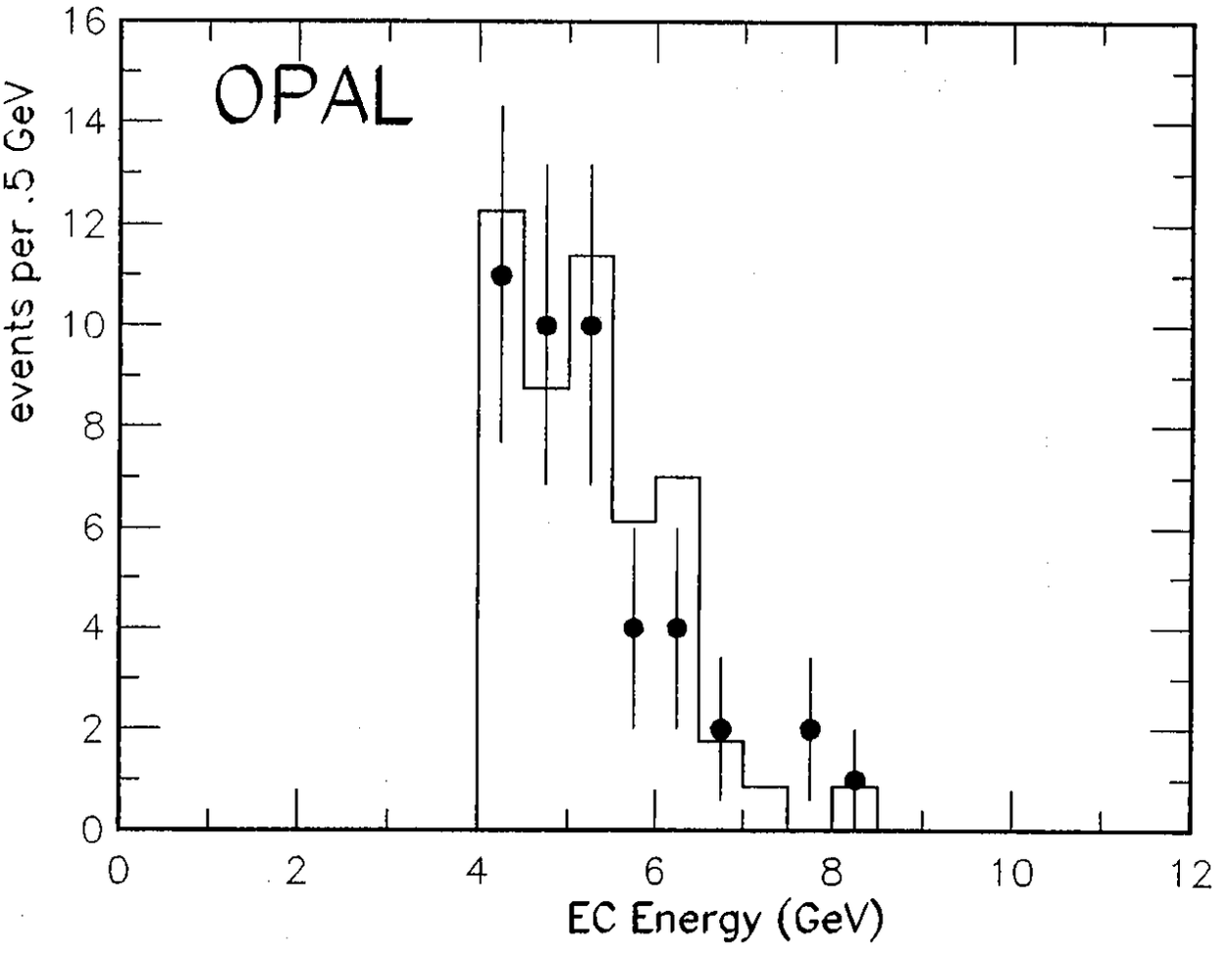

FIGURE 3

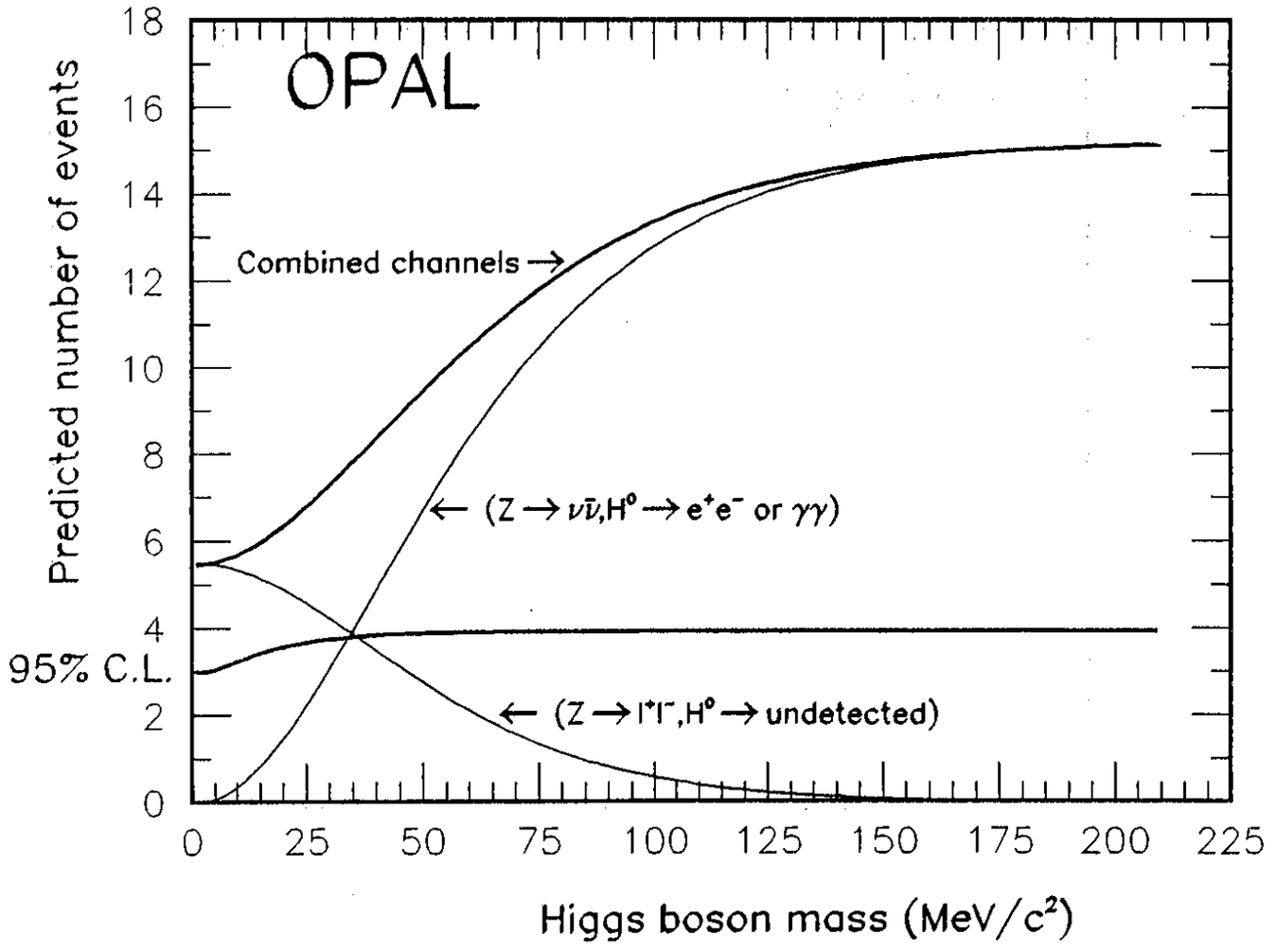

FIGURE 4

Imprimé au CERN. Prix : 0.65 Fr.